Current Research in Food Science 5 (2022) 1365–1378

Contents lists available at ScienceDirect

Current Research in Food Science

journal homepage: www.sciencedirect.com/journal/current-research-in-food-science

Intestinal microbiomics and liver metabolomics insights into the preventive effects of chromium (III)-enriched yeast on hyperlipidemia and hyperglycemia induced by high-fat and high-fructose diet

Mei-Ting Wang [a,b,1], Wei-Ling Guo [a,d,1], Zi-Yi Yang [a,b], Feng Chen [a], Tian-Tian Lin [a,e], Wen-Long Li [a,b], Xu-Cong Lv [a,b,*], Ping-Fan Rao [a], Lian-Zhong Ai [c], Li Ni [a,b,**]

[a] Institute of Food Science and Technology, College of Biological Science and Technology, Fuzhou University, Fuzhou, Fujian, 350108, China
[b] Food Nutrition and Health Research Center, School of Advanced Manufacturing, Fuzhou University, Jinjiang, Fujian, 362200, China
[c] School of Medical Instruments and Food Engineering, University of Shanghai for Science and Technology, Shanghai, 200093, China
[d] International Joint Research Center for Probiotics & Gut Health, School of Food Science and Technology, Jiangnan University, Wuxi, Jiangsu, 214122, China
[e] School of Clinical Medicine, Fujian Medical University, Fuzhou, Fujian, 350122, China

ARTICLE INFO

Handling editor: Dr. Yeonhwa Park

Keywords:
Chromium (III)-Enriched yeast
Hyperlipidemia
Hyperglycemia
Intestinal microbiota
Liver metabolomics

ABSTRACT

In recent years, organic chromium (III) supplements have received increasing attentions for their low toxicity, high bioavailability and wide range of health-promoting benefits. This study aimed to investigate the preventive effects of chromium (III)-enriched yeast (YCr) on high-fat and high-fructose diet (HFHFD)-induced hyperlipidemia and hyperglycemia in mice, and further clarify its mechanism of action from the perspective of intestinal microbiomics and liver metabolomics. The results indicated that oral administration of YCr remarkably inhibited the aberrant elevations of body weight, blood glucose and lipid levels, hepatic cholesterol (TC) and triglyceride (TG) levels caused by HFHFD. Liver histological examination showed that oral YCr intervention inhibited HFHFD induced liver lipid accumulation. Besides, 16S rDNA amplicon sequencing showed that YCr intervention was beneficial to ameliorating intestinal microbiota dysbiosis by altering the proportion of some intestinal microbial phylotypes. Correlation-based network analysis indicated that the key intestinal microbial phylotypes intervened by YCr were closely related to some biochemical parameters associated with glucose and lipid metabolism. Liver metabolomics analysis revealed that dietary YCr intervention significantly regulated the levels of some biomarkers involved in purine metabolism, glycerophospholipid metabolism, citrate cycle, pyrimidine metabolism, glycerophospholipid metabolism, phenylalanine, tyrosine and tryptophan biosynthesis, and so on. Moreover, dietary YCr intervention regulated the mRNA levels of key genes associated with glucose, cholesterol, fatty acids and bile acids metabolism in liver. These findings suggest that dietary YCr intervention has beneficial effects on glucose and lipid metabolism by regulating intestinal microbiota and liver metabolic pathway, and thus can be served as a functional component to prevent hyperlipidemia and hyperglycemia.

1. Introduction

Due to unhealthy dietary habits and lifestyle, obesity, hyperglycemia and dyslipidemia and atherosclerosis have gradually become serious problems threatening human health worldwide. Among them, dyslipidemia is a chronic metabolic disease chiefly characterized by elevated blood lipid levels, which is significantly positively correlated with the increased incidence of cardiovascular diseases (Çakır et al., 2022). It is estimated that by 2022, about 78 million people worldwide will suffer from chronic metabolic diseases with dyslipidemia (Chalasani et al., 2018). Dyslipidemia remarkably elevates the risk of hyperglycemia and diabetes (Gujjala et al., 2016). Excessive energy intake is a vital factor in

* Corresponding author. Institute of Food Science and Technology, College of Biological Science and Technology, Fuzhou University, Fuzhou, Fujian, 350108, China.
** Corresponding author. Institute of Food Science and Technology, College of Biological Science and Technology, Fuzhou University, Fuzhou, Fujian, 350108, China.
E-mail addresses: xucong1154@163.com (X.-C. Lv), nili@fzu.edu.cn (L. Ni).
[1] Co-first authors: Mei-Ting Wang and Wei-Ling Guo contributed equally to this study.

https://doi.org/10.1016/j.crfs.2022.08.015
Received 6 May 2022; Received in revised form 20 August 2022; Accepted 22 August 2022
Available online 28 August 2022

dyslipidemia and hyperglycemia (Guo et al., 2018). Accumulating evidence demonstrates that high-fat and high-fructose diet (HFHFD) consumption may accelerate the occurrence of hyperglycemia and dyslipidemia by increasing the intake amount of fatty acids and destroying the metabolic function of the liver (Savva et al., 2022). Although various drugs have been widely used to treat hyperglycemia and dyslipidemia, most of the therapeutic drugs have various side effects. Therefore, the development of natural products with strong ameliorative effects is an effective strategy to prevent the occurrence and pathological process of hyperglycemia and dyslipidemia.

Chromium (III), as an essential trace element, is an important part of human glucose tolerance factor and can improve hyperglycemia by ameliorating glucose tolerance and lowering fasting blood glucose (Sundaram et al., 2013). Chromium (III) deficiency increases the risk of glucose and lipid metabolism disorders (Li et al., 2019). Dietary chromium (III) supplementation can increase insulin sensitivity and glucose tolerance, thereby reducing the risk of hyperglycemia and atherosclerotic complications. Nevertheless, inorganic chromium (III) is difficult to be absorbed in gastrointestinal tract and may be harmful to human health because it can be oxidized into toxic hexavalent chromium (Guo et al., 2020a; Quievryn et al., 2003). Compared to inorganic chromium (III), organic chromium (III) has attracted increasing attention recently because of its relatively low toxicity, high bioavailability and wide range of health benefits (Jaroslav et al., 2009). Some organic chromium (III) supplements were synthesized and their pharmacological properties were evaluated, such as chromium propionate, chromium histidinate and polysaccharides-chromium (Guo et al., 2020a; Hayat et al., 2020). For the past few years, the enrichment of trace element by brewer's yeast has been extensively explored, including selenium-enriched yeast (Zhang et al., 2018), S-iron-enriched yeast (Zhang et al., 2021), zinc-enriched yeast (Maares et al., 2022) and chromium (III)-enriched yeast (YCr) (Król et al., 2011). YCr is a chromium-rich (III) yeast preparation with no adverse physiological effects reported in a series of animal toxicological studies or human clinical efficacy trials (Hou et al., 2019; Shan et al., 2020). Dietary supplementation with YCr has previously been reported to better control the fasting blood glucose, serum cholesterol, triglycerides concentrations and blood pressure in patients with type 2 diabetes (Hosseinzadeh et al., 2013). However, few researches have been performed to investigate and compare the beneficial effects of dietary YCr and Cr supplementation on glucose and lipid metabolism profile *in vivo*.

It is commonly accepted that intestinal microbiome plays a crucial role in the occurrence of hyperglycemia and dyslipidemia caused by excessive energy intake. The intestinal microbiome, known as the second genome of the human body, may influenced by diet, lifestyle and genotypic milieu. More and more evidences have shown that long-time consumption of high energy diet alters the intestinal microbial composition and reduces the protein expression of zonula occludens (ZO), and then destroys liver metabolism functions (Chen et al., 2021). It was previously reported that excessive energy intake resulted in a decrease in the abundance of Bacteroidetes and an increase in the abundance of Firmicutes in the gut of mice (Miyamoto et al., 2019). In addition, long-term high energy diet consumption not only changes the composition of intestinal flora, but also affects its metabolites, including short-chain fatty acids (SCFAs), bile acids (BAs), as well as branched-chain amino acids (BCAAs) (Guo et al., 2018). Significant increases in the abundance of *Lactobacillus*, *Bifidobacterium*, *Faecalibacterium* and *Akkermansia* are known to improve intestinal barrier and alleviate liver damage (Chen et al., 2020; Lv et al., 2021). Accumulating evidence supports the beneficial role of SCFAs in liver metabolism function (Canfora et al., 2015). Long-time western diet intake may change the liver metabolomic profiling, thus relieve the development of dyslipidemia (Guo et al., 2020c). There is a close correlation between diet and intestinal microbiome, but how chromium (III)-enriched yeast (YCr) affects the intestinal microbial composition and liver metabolic function is still unknown. The modulation of intestinal microbiome and liver metabolome might be partially responsible for the hypolipidemic and hepatoprotective effects of YCr intervention.

In this study, we explored the possible mechanism of action of YCr intervention against hyperglycemia and dyslipidemia in mice through intestinal microbiomics and liver metabolomics, coupled with liver gene transcription analysis. In addition, the relationship between intestinal microbiota features and biochemical parameters was revealed through statistical correlation analysis, providing scientific references for the development of functional foods for people at risk of hyperglycemia and dyslipidemia.

2. Materials and methods

2.1. Chromium (III)-enriched yeast and chemical reagents

Chromium (III)-enriched yeast (*Saccharomyces cerevisiae* Angel strain) used in this study was purchased from Angel Yeast Co., Ltd. (Yichang, Hubei, China), and the chromium content in chromium (III)-enriched yeast was 1000 ppm. Portable blood glucometers were obtained from Omron Co., Ltd. (Suzhou, Jiangsu, China). Other chemicals were purchased from Shanghai Sangon Biotech Co., Ltd. (Shanghai, China) unless otherwise noted.

2.2. Animal experimental design

Male Kunming mice without specific pathogens (n = 48, six-week-old) were obtained from Jinan Jinfeng Experimental Animal Co., Ltd. (Jinan, Shandong, China). All mice were kept in a laboratory of specific pathogen free (SPF) grade (temperature 22 ± 2 °C, humidity 58 ± 2%, 12-h/12-h light/dark cycle), and sterile diets and water were provided *ab libitum*. After 7 days acclimatization period, all mice were randomly assigned into the following six groups: (1) the control group (n = 8, fed with a standard chow diet and orally gavaged with 0.2 mL sterile physiological saline once a day); (2) the model group (n = 8, fed with a high-fat and high-fructose diet [HFHFD] and orally gavaged with 0.2 mL sterile physiological saline once a day); (3) the YCr–H group (n = 8, fed with a HFHFD and orally gavaged with YCr [32 mg/kg b.w./day, the amount of Cr is 32 μg/kg b.w./day]); (4) the YCr-L group (n = 8, fed with a HFHFD and orally gavaged with YCr [8 mg/kg b.w./day, the amount of Cr is 8 μg/kg b.w./day]); (5) the Cr–H group (n = 8, fed with a HFHFD and orally gavaged with $CrCl_3$ [96 μg/kg b.w./day, the amount of Cr is equal to that of the YCr–H group]); (6) the Cr-L group (n = 8, fed with a HFHFD and orally gavaged with $CrCl_3$ [24 μg/kg b.w./day, the amount of Cr is equal to that of the YCr-L group]). YCr and $CrCl_3$ were dissolved in physiological saline and intragastrically administered daily at 8 a.m. for eight weeks. The dosages used in the present study were selected according to the daily consumption of chromium recommended by Chinese Nutrition Society (50–200 μg), and the conversion between human clinical dose and the body surface area of mouse. Detailed ingredients of standard chow diet and HFHFD were available in Table S1.

After 8 weeks' intervention, all mice were euthanized after 12 h of fasting, fasting blood glucose and oral glucose tolerance test were measured according to our previous study (Guo et al., 2020b). Blood samples and cecal contents were collected separately from each mouse. The blood samples were stored at room temperature for 30 min, and then centrifuged at 3000 g for 10 min to obtain serum and then stored at −20 °C for storage. Immediately after dissection, the liver of each mouse was weighed, then snap frozen in liquid nitrogen and finally stored at −80 °C. Animal experiments were carried out according to the guidelines of the Laboratory Animal Welfare and approved by the Committee of Animal Ethics (FZU-FST-2019-038).

2.3. Biochemical measurements of the serum and liver samples

Serum total cholesterol (TC), triglyceride (TG), low-density lipoprotein cholesterol (LDL-C) and high-density lipoprotein cholesterol

(HDL-C) levels were determined using the blood automatic biochemical analyzer (Hitachi, Tokyo, Japan). The TC, TG, glycogen levels in the liver, and the TC, TG, bile acids (BAs) levels in the feces were determined by the corresponding commercial kits (Jiancheng, Nanjing, China) following the operating instructions.

2.4. Histopathologic evaluation of liver

Histopathological examination was conducted using fresh liver sections fixed in 4% paraformaldehyde and dehydrated using ethanol solutions. Following embedding in paraffin, the sections were cut into 5 μm thick sections and the photos were taken with a digital camera microscope (Nikon, Tokyo, Japan) after the sections were stained with hematoxylin and eosin.

2.5. Analysis of fecal SCFAs by gas chromatograph (GC)

Fecal samples were collected individually following the Standard Operating Procedure (SOP) of self-collection (http://www.microbiome-standards.org). Fecal SCFAs concentrations were extracted and determined according to a method from a previous study (Zhang et al., 2020). 100 mg dried fecal powder was resuspended in 1 mL of distilled water and vortexed for 2 min. Then, 600 μL of the supernatant of the fecal slurry was acidified with 20% (v/v) H_2SO_4. After vortexing for 1 min, 500 μL of n-butanol was added to the mixture and vortexed for 2 min. The supernatant was filtered through a 0.22 μm filter membrane for sample injection. Agilent 7890B GC system (Agilent Technologies, Santa Clara, CA) equipped with a DB-FFAP capillary column (30 m × 0.32 mm i.d., 0.25 μm film thickness, Agilent, Santa Clara, USA) was used for component separation and detection of the fecal SCFAs concentrations.

2.6. 16S rRNA amplicon high throughput sequencing

Bacterial genomic DNAs of cecal contents were extracted using fecal DNA extraction kit (MoBio, USA). Bacterial genomic DNAs were used to amplify the V3–V4 hypervariable region of the 16S rRNA gene with the forward primer 341 F and the reverse primer 806 R (Zhang et al., 2020). Validated libraries were used for sequencing on the Illumina MiSeq platform at Shanghai Majorbio Co., Ltd. (Shanghai, China). The quality control and clustering results were analyzed by QIIME 2.0 software (version 2019.7). The optimized sequences were clustered with 97% similarity and compared with the GreenGenes database (version 13.8) to identify the bacterial phylotypes at the genus level. Principal component analysis (PCA) and hierarchical clustering plot was carried out by the SIMCA-14.1 software (UMETRICS, Sweden). Differential abundance analyses of intestinal microbial phylotypes between different experimental groups at the genus level were assessed using STAMP software (Ver. 2.1.3) based on Welsh's *t*-test. Correlation analysis was performed based on Spearman's rank correlation, and the correlations between the key intestinal microbial phylotypes and biochemical parameters were visualized by heatmap and network through R (Ver. 3.3.3) and Cytoscape software (Ver. 3.9.0), respectively.

2.7. Metabolomics detection of liver

Untargeted metabolomics detection was performed to analyse the global liver metabolites. In brief, liver sample (25 mg) was mixed with 400 μL of 70% methanol water, vortexed for 3 min and sonicated for 10 min in an ice water bath. Then, the mixture was centrifuged (10000 g, 4 °C) for 10 min, and the supernatant was collected for analysis. The sample extracts were analyzed using an UPLC-QTOF/MS system (Agilent 1290 Infinity UPLC equipped with Agilent 6530 MS). The analytical conditions were as follows: UPLC column, Waters ACQUITY UPLC BEH Amide (1.7 μm, 2.1 mm × 100 mm); column temperature, 40 °C; flow rate, 0.4 mL/min; injection volume, 2 μL; solvent system, water (25 mM ammonium formate/0.4% ammonia): acetonitrile; gradient program, 10:90 (V/V) at 0 min, 40:60 (V/V) at 9.0 min, 60:40 (V/V) at 10.0 min, 60:40 (V/V) at 11.0 min, 10:90 (V/V) at 11.1 min, 10:90 (V/V) at 15.0 min. The ESI source operation parameters were as follows: source temperature 500 °C; ion spray voltage 5500 V (ESI+), −4500 V (ESI-); ion source gas I, gas II, and curtain gas were set at 55, 60, and 25.0 psi, respectively. MPP software (Agilent, CA, USA) was used to convert and process the MS raw data for peak detection, alignment and identification. SIMCA 15.0 software was used to perform multivariate statistical analysis. Metabolites of significant difference between the model and YCr groups were selected by OPLS-DA (VIP value > 1.0, $P < 0.05$). The selected metabolites were identified by HMDB database. Finally, pathway analysis was performed for metabolites with significant difference using MetaboAnalyst 5.0 online platform.

2.8. Reverse transcription quantitative PCR (RT-qPCR) analysis

The total RNA of mouse liver was extracted using a RNA extraction kit of Takara Bio-Technology Co., Ltd. (Beijing, China), and then reverse-transcribed into cDNA using a commercial cDNA kit with gDNA Eraser (Takara, Beijing, China). qPCR was completed in StepOne Plus Real-Time quantitative PCR System (Applied Biosystems, Foster City, CA, USA) with SYBE Green Ex Taq™ II (Takara, Beijing, China). The mRNA expression levels were normalized to β-Actin gene. The qPCR data were analyzed according to $2^{-\Delta\Delta CT}$ standard method. Table 1 showed the primers used in the current study.

2.9. Statistical analysis

To calculate the significance of differences between groups, the data were analyzed using one-way ANOVA with GraphPad Prism (Ver. 7.0) software followed by Duncan's multiple range test. The threshold for differences to be statistically significant was $P < 0.05$.

3. Results

3.1. Effects of YCr intervention on body growth performance and fat mass

The changes of body growth performance and body weight gain were shown in Fig. 1A–B. At the early stage of the experiment, there was no statistically significant difference in body weight among different groups (Fig. 1A). After eight weeks of HFHFD feeding, the average body weight of mice in the model group was significantly higher than that of the control group (Fig. 1A), suggesting that excessive intake of fat and fructose may impair the metabolic capabilities of body. Interestingly, the abnormal increases in body weight caused by HFHFD feeding were significantly alleviated by YCr intervention and Cr intervention ($P < 0.05$) (Fig. 1B). In addition, oral administration of YCr and Cr could significantly inhibit the abnormal increase of liver index in mice fed with HFHFD ($P < 0.05$) (Fig. 1C).

3.2. Effects of YCr intervention on serum biochemical parameters

As shown in Fig. 1D-I, HFHFD consumption for eight weeks resulted in abnormal increases in blood glucose, AUC and serum TC, TG and LDL-C levels, compared with the control group ($P < 0.05$), but there was no significant difference in serum HDL-C concentration ($P > 0.05$). Treatment of HFHFD-fed mice with YCr significantly alleviated lipid metabolism disturbance by decreasing the serum levels of TC, TG and LDL-C, and increasing serum level of HDL-C, indicating that YCr intervention may have a significant hypolipidemic effect. Moreover, dietary YCr supplementation profoundly restored the biochemical parameters of glucose homeostasis by reducing fasting blood glucose level and enhancing fasting glucose tolerance, indicating that YCr intervention also has a significant hypoglycemic effect. Besides, in comparison to inorganic chromium (Cr), YCr intervention has an advantage at enhancing fasting glucose tolerance and reducing serum TC levels,

Table 1
Primer sequences for quantitative real-time PCR.

Gene	Forward primer (5′–3′)	Reverse primer (5′–3′)
Glut4	ACCATAGGAGCTGGTGTGGTCAAT	GACCCATAGCATCCGCAACA
Pepck	GTTCCCAGGGTGCATGAAAG	AGGGCGAGTCTGTCAGTTCAA
G6Pase	AATCTCCTCTGGGTGGC	TGCTGTAGTAGTCGGTGTCC
Gk	TCCCTGTAAGGCACGAAGA	GAGAAGTCCCACGATGTTGTT
Gp	GAGCACCCAATGACTTTAACCTTC	TATTCTCAGCCAGGTTCCGGT
FBPase	TGTGGGCTCCACCTGCCTGCACCTTTAGTC	TTTGATCGCGGTGCAGAGCGAATTCAGCAG
Akt	GAGCATCATCCCTGGGTTAC	CTCCTTCACAATGGCTACG
Ppar-α	CCTGGAAAGTCCCTTATCT	GCCCTTACAGCCTTCACAT
Cd36	ACTTGGGATTGGAGTGGTGATGT	GGATACCTGCAGTTTGAGCCA
Hsl	GCCGGTGACGCTGAAAGTGGT	CGCGCAGATGGGAGCAAGAGGT
Acsl1	CACTTCTTGCCTCGTTCCAC	GTCGTCCCGCTCTATGACAC
Fxr	GGCAGAATCTGGATTTGGAATCG	GCCCAGGTTGGAATAGTAAGACG
Cpt-1	TCCATGCATACCAAAGTGGA	TGGTAGGAGAGCAGCACCTT
Lxr	CTGATTCTGCAACGGAGTTGT	GACGAAGCTCTGTCGGCTC
Acat2	AAAGCGTAACATCTCAGCAAA	AACAGGAGCCCTTCAGTG
Acc1	GCCATCCGGTTTGTTGTCA	GGATACCTGCAGTTTGAGCCA
Srebp-1c	GCCGGCGCCATGGACGAGCTGG	CAGGAAGGCTTCCAGAGAGGAG
β-Actin	ACGTCGACATCCGCAAAGACCTC	TGATCTCCTTCTGCATCCGGTCA

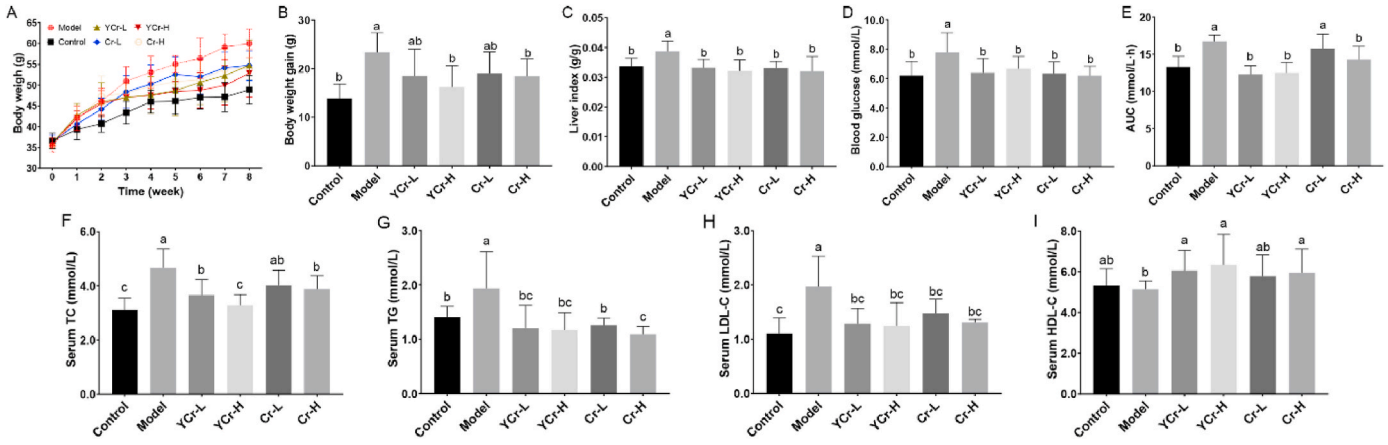

Fig. 1. Effects of YCr intervention on the body weight growth trend (A), body weight gain (B), liver index (C), and serum biochemical parameters (blood glucose, AUC, TC, TG, LDL-C and HDL-C) (D–I) in HFHFD-fed mice. Columns with different letters are statistical significance by Duncan's multiple range test ($P < 0.05$).

suggesting that YCr appeared to be more effective than inorganic chromium (Cr) in improving glucose and lipid metabolism in mice fed with HFHFD.

3.3. Effects of GLP-Cr intervention on liver biochemical and histological features

To evaluate the effects of YCr and Cr interventions on liver glucose and lipid metabolism, the hepatic TC, TG and glycogen levels were detected by commercial kits (Fig. 2A–C). Compared with the control group, the hepatic TC, TG levels were significantly increased in the model group, and the hepatic glycogen levels were significantly reduced ($P < 0.05$). Furthermore, histopathological examination of liver by H&E staining showed that the mice of the control group had evident liver lobule (Fig. 2D), round central nucleus, distinct cytoplasm and cell borders, but there were obvious lipid droplets in liver of mice of the model group. However, compared with the model group, both high-dose YCr intervention and Cr intervention can significantly reduce excessive fat accumulation in the liver, and the liver characteristics of the YCr–H and Cr–H were equivalent to those of the control group. Compared with the Cr–H group, liver histological morphology of mice in the YCr–H group was more similar to that of the control group, indicating that the protective effect of YCr on liver was superior to that of Cr intervention.

3.4. Effects of YCr intervention on the fecal biochemical parameters

As shown in Fig. 3, the fecal TC level was remarkably increased in mice of the model group, compared with the control group ($P < 0.05$), but there were no significant difference in fecal TG and BAs levels ($P > 0.05$). After 8 weeks of intervention with YCr and Cr, the levels of fecal TC, TG and BAs levels were significantly higher than those in the model group, especially the high-dose YCr intervention ($P < 0.05$). Intestinal microbiota-derived SCFAs that exert a number of actions on host cells, especially for ameliorating glycolipid metabolism homeostasis. As shown in Fig. 4, compared with the control group, the fecal levels of acetic, n-butyric, isobutyric, n-valeric and isovaleric acids in mice fed with HFHFD were remarkably reduced after 8 weeks' experiment ($P < 0.05$), but there was no significant difference in the fecal levels of propionic acid ($P > 0.05$). In contrast, in the HFHFD-fed mice, oral administration of YCr or Cr significantly increased the amount of these substances in feces ($P < 0.05$).

3.5. Effects of YCr intervention on the composition of intestinal microflora

The overall changes of intestinal microbiota were analyzed by PCA and hierarchical cluster analysis. The PCA score plots illustrated that the model group was obviously separated from the control group on the first principal component axis (PC[1]) (Fig. 5A and B), indicating that HFHFD feeding could induce the disorder of the composition of

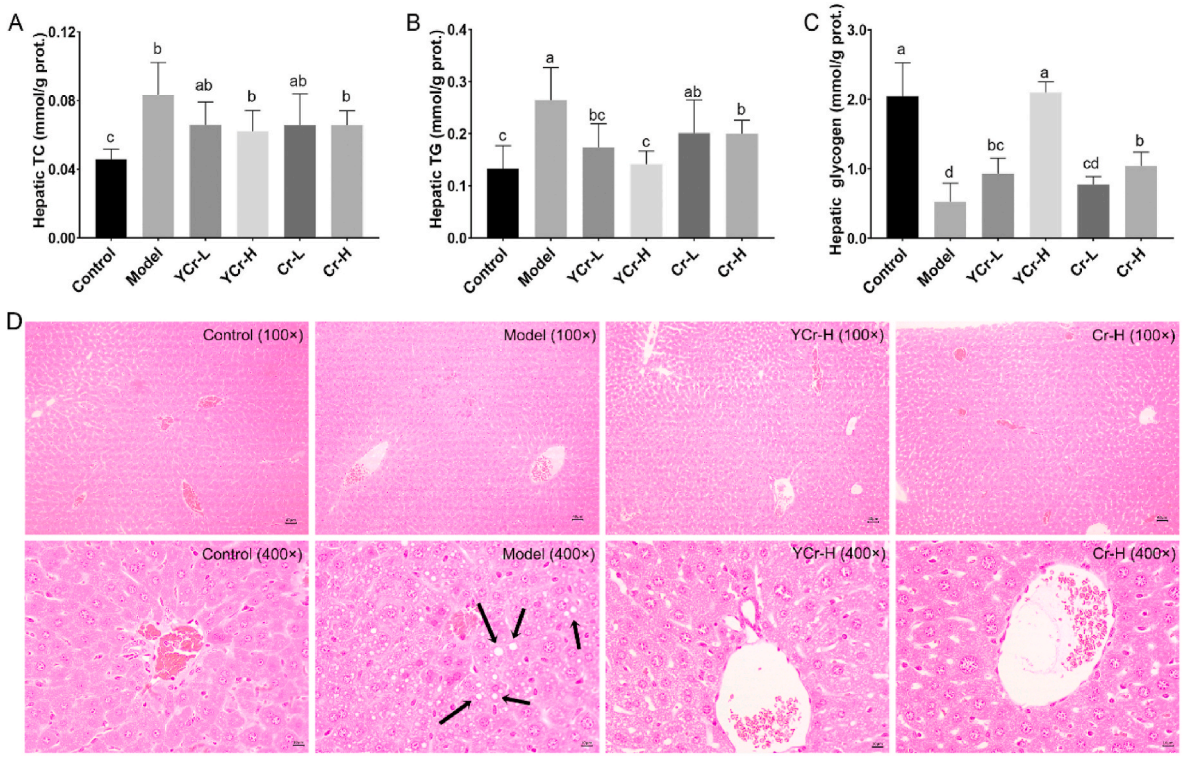

Fig. 2. Effects of YCr intervention on the hepatic levels of TC (A), TG (B), glycogen (C) and liver histopathological features in HFHFD-fed mice (D). Columns with different letters are statistical significance by Duncan's multiple range test ($P < 0.05$).

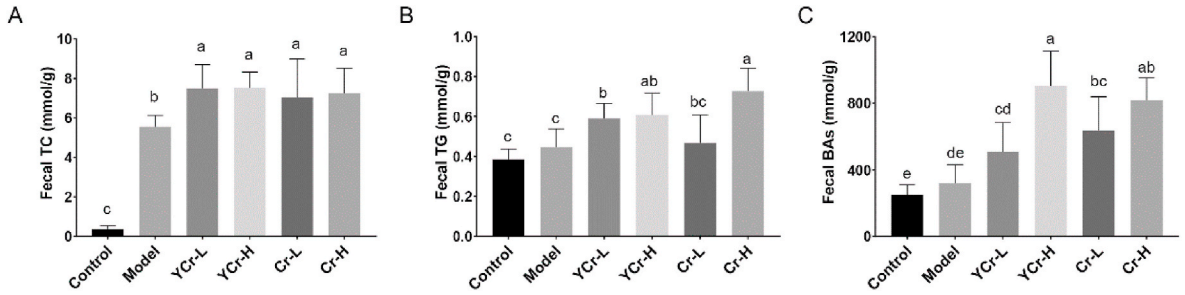

Fig. 3. Effects of YCr intervention on the fecal levels of TC (A), TG (B), and BAs (C) in HFHFD-fed mice. Columns with different letters are statistical significance by Duncan's multiple range test ($P < 0.05$).

intestinal microbiota. The Cr–H group could be clearly separated from the model group on the second principal component axis (PC[2]) (Fig. 5A), and the YCr–H group could be clearly separated from the model group on the third principal component axis (PC[3]) (Fig. 5B), suggesting that the intestinal microbiota composition were evidently regulated by high-dose YCr and Cr interventions to a certain extent. The hierarchical clustering tree based on the relative abundance of OTUs also indicated that oral administration of YCr or Cr could obviously influence the composition of intestinal microbiota in mice with excessive fat and fructose intake (Fig. 5C).

Furthermore, differential analysis of the relative abundance at the genus level among different experimental groups revealed the effects of HFHFD feeding and YCr intervention on the composition of intestinal microflora (Fig. 6). As compared with the control group, mice fed with HFHFD were characterized by elevated proportions of norank_f_*Desulfowibrlionaceae*, *Lachnospiraceae*_UCG-006, *Coprobacillus*, UBA1819, *Intestinimonas*, *Parabacteroides*, *Holdemania*, unclassified_o_Bacteroidales, *Clostridium_innocuum* group and unclassified_c_Clostridia, but lower abundances of *Lachnospiraceae*_NK4A136_group, unclassified_f_*Lachnospiraceae*, *Lactobacillus*, norank_f_*Lachnospiraceae*, *Candidatus_Saccharimonas*, *Roseburia*, norank_o_*Clostridia*_UCG-014, A2, *Enterorhabdus*, *Eubacterium_siraeum*_group, *Anaerotruncus*, norank_f_UCG-010, *Ruminococcus*, *Candidatus_Arthromitus*, *Christensenellaceae*_R-7_group, *Monoglobus*, *Butyricicoccus* and norank_o_RF39, norank_o_Clostridia_vadinBB60 group. As expected, high-dose YCr intervention remarkably increased the proportions of *Eubacterium_nodatum*_group, unclassified_c_Clostridia, but remarkably reduced the relative abundances of norank_f_Muribaculaceae, A2, Family_XIII_UCG-001, *Marvinbryantia*, norank_f_Erysipelatoclostridiaceae, *Ruminiclostridium* in HFHFD-fed mice. However, high-dose Cr intervention significantly increased the proportions of *Escherichia-Shigella*, *Eubacterium_brachy*_group, *Weissella*, norank_o_Oscillospirales, norank_o_Chloroplast, but significantly reduced the relative abundances of *Parabacteroides*, *Odoribacter*, unclassified_f_Muribaculaceae, norank_o_Clostridia_vadinBB60_group and *Ralstonia*.

3.6. Correlations of the key microbial phylotypes with biochemical parameters

To investigate the relationship between the key microbial phylotypes

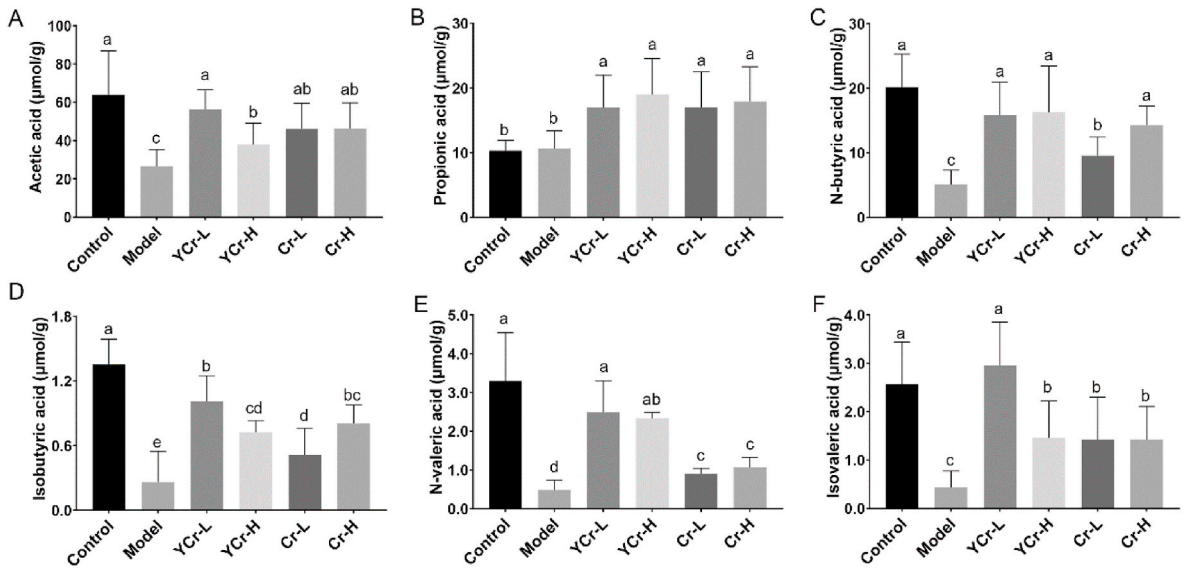

Fig. 4. Effects of YCr intervention on the fecal levels of acetic acid (A), propionic acid (B), n-butyric acid (C), isobutyric acid (D), n-valeric acid (E), and isovaleric acid (F) in HFHFD-fed mice. Columns with different letters are statistical significance by Duncan's multiple range test ($P < 0.05$).

and biochemical parameters, Spearman correlation analysis was conducted out (Fig. 7A and Fig. 7B). It is worth noting that norank_f_*Erysipelatoclostridiaceae*, *Marvinbryantia*, A2, Family_XIII_UCG-001, *Ruminiclostridium* and norank_f_*Muribaculaceae* were found to be positively associated with the serum biochemical parameters, including serum TC, TG, LDL-C and HDL-C, but negatively associated with hepatic glycogen, fecal butyrate and valerate levels. By contrast, unclassified_d_Bacteria, unclassified_c_Clostridia, and *Eubacterium_nodatum*_group showed positive associations with the hepatic glycogen levels and fecal SCFAs and BAs levels, but negative associations with the serum biochemical parameters including HDL-C, TG, LDL-C and TC. In addition, the potential correlation between the key intestinal microbial phylotypes and the parameters associated with glucose and lipid metabolism were remarkably regulated by Cr intervention were also analyzed (Fig. 7C–D). *Ralstonia*, norank_o_Clostridia_vadinBB60 group, unclassified_f_Muribaculaceae, *Parabacteroides* showed positive associations with the serum HDL-C, TG, LDL-C, TC and fasting blood glucose, body weight gain, but negative associations with fecal TG and butyrate. However, *Escherichia-Shigella*, *Weissella*, *Eubacterium brachy* group exhibited negative associations with the serum LDL-C and blood glucose levels, but positive associations with the fecal SCFAs, fecal TG and hepatic glycogen levels.

3.7. Effects of YCr intervention on liver metabolome

PCA and PLS-DA score plots of mouse liver metabolites allowed to show a significant differential metabolic profiling between different experimental groups (Fig. 8A&B and 9A&B), indicating that HFHFD feeding and YCr intervention significantly affected the function of liver metabolism. Impressively, OPLS-DA score plots revealed a clear segregation between the model and YCr groups (Figs. 8C and 9C), suggesting YCr treatment greatly improved the liver impairment in HFHFD-fed mice. The OPLS-DA loadings S-plots showed significant differences in liver metabolites (potential biomarkers) between the model and YCr groups (VIP >1.0 and $P < 0.05$) (Figs. 8D and 9D). A total of 150 potential biomarkers between the model and YCr groups were successfully obtained, including 81 liver metabolites were obviously up-regulated and 69 liver metabolites were obviously down-regulated by YCr intervention (Figs. 8E and 9E).

Based on MetaboAnalyst 5.0 online platform, we analyzed the effect of YCr treatment on the metabolic pathway in liver (Figs. 8F and 9F). The results of KEGG pathway enrichment analysis revealed that arginine biosynthesis, purine metabolism, alanine, aspartate and glutamate metabolism, retinol metabolism, inositol phosphate metabolism, phenylalanine, tyrosine and tryptophan biosynthesis, glycerophospholipid metabolism, phenylalanine metabolism, arachidonic acid metabolism, glyoxylate and dicarboxylate metabolism, glycolysis/gluconeogenesis, pyruvate metabolism, citrate cycle, galactose metabolism, steroid hormone biosynthesis, pyrimidine metabolism and phenylalanine were significantly altered by YCr intervention (Figs. 8F and 9F).

Furthermore, PCA, PLS-DA and OPLS-DA results showed that liver metabolic profiles were obviously altered in HFHFD-fed mice with Cr intervention (Figs. S1A–C, S2A-C). As shown in Fig. S1 D&E and Fig. S2 D&E, compared to the model group, 20 liver metabolites were significantly up-regulated and 24 liver metabolites were significantly down-regulated by Cr intervention. Subsequently, KEGG pathway enrichment analysis was carried out to explore the metabolic pathways significantly altered by Cr intervention in HFHFD-fed mice. In detail, compared to the model group, purine metabolism, cysteine and methionine metabolism, glycerophospholipid metabolism, glycerolipid metabolism, pyrimidine metabolism, inositol phosphate metabolism, glyoxylate and dicarboxylate metabolism, pyruvate metabolism, citrate cycle and galactose metabolism were enriched to be the main metabolic pathways significantly altered by Cr intervention (Fig. S1F and Fig. S2F).

3.8. Effects of YCr intervention on the liver mRNA levels

In order to clarify the possible mechanism of hypoglycemic and hypolipidemic effects of YCr intervention, the mRNA levels of genes responsible for glucose and lipid metabolism in liver were detected by qPCR. Although there was no statistical significance in the mRNA levels of sodium taurocholate cotransporting polypeptide (*Ntcp*), diacylglycerol O-acyltransferase 2 (*Dgat2*), acyl-CoA oxidase 1 (*Acox1*), glucose transporter 4 (*Glut4*), fructose-1,6-bisphosphatase (*FBPase*), apolipoprotein E (*ApoE*), glucokinase (*Gk*), carnitine palmitoyltransferase-1 (*Cpt-1*) between the model and control groups ($P > 0.05$), the mRNA levels of cholesterol 7-alpha hydroxylase (*Cyp7a1*), protein kinase B (*Akt*) and low density lipoprotein receptor (*Ldlr*) were significantly down-regulated in mice fed with HFHFD, compared with the control group (Fig. 10). On the contrary, the mRNA levels of fatty acid transport protein-1 (*Fatp-1*), long-chain acyl-CoA synthetase 1

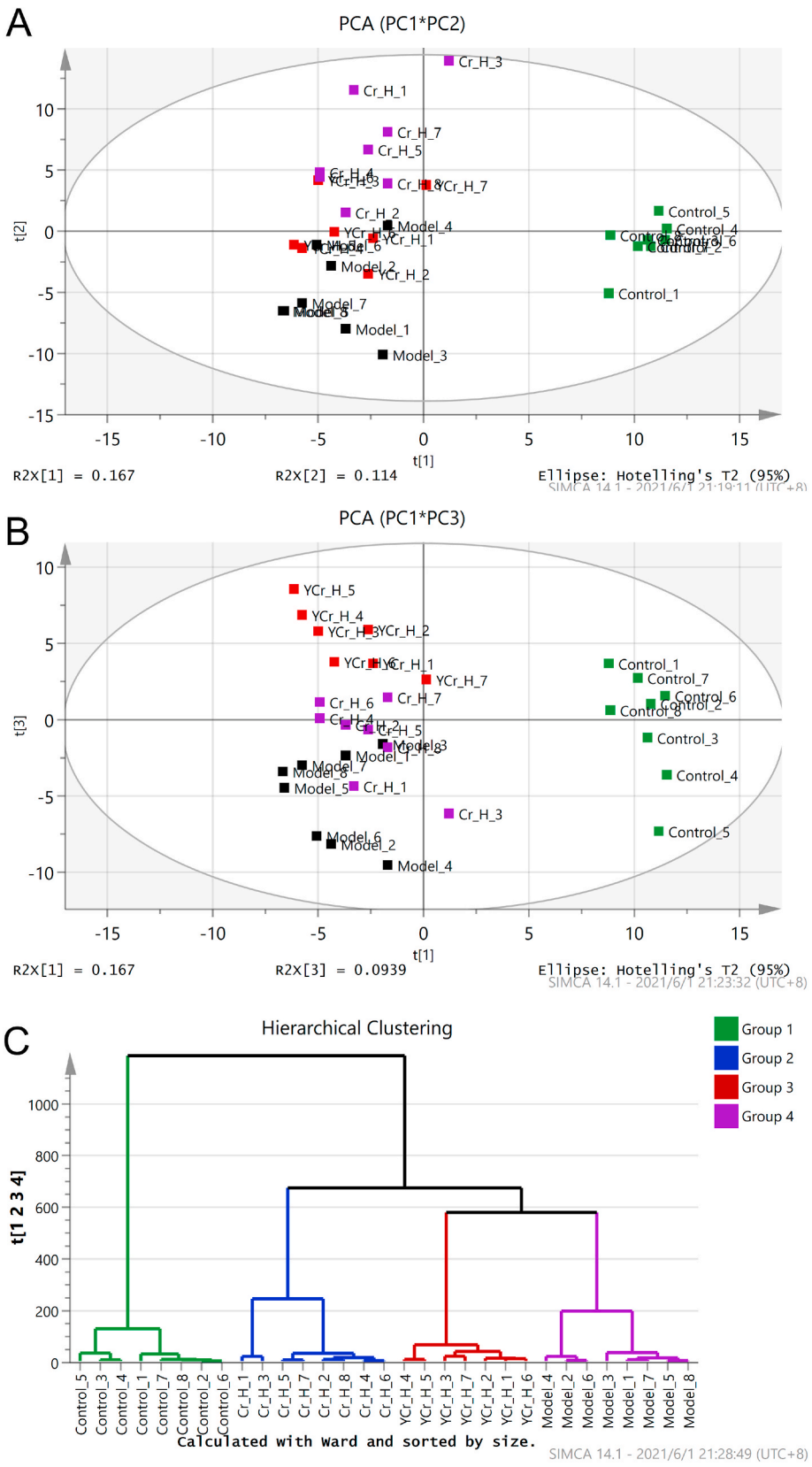

Fig. 5. Principal component analysis (PCA) score plots and hierarchical clustering analysis of intestinal microbiota of different experimental groups. Score plots of PCA (PC1 × PC2) (A) and (PC1 × PC3) (B); hierarchical clustering plot (C).

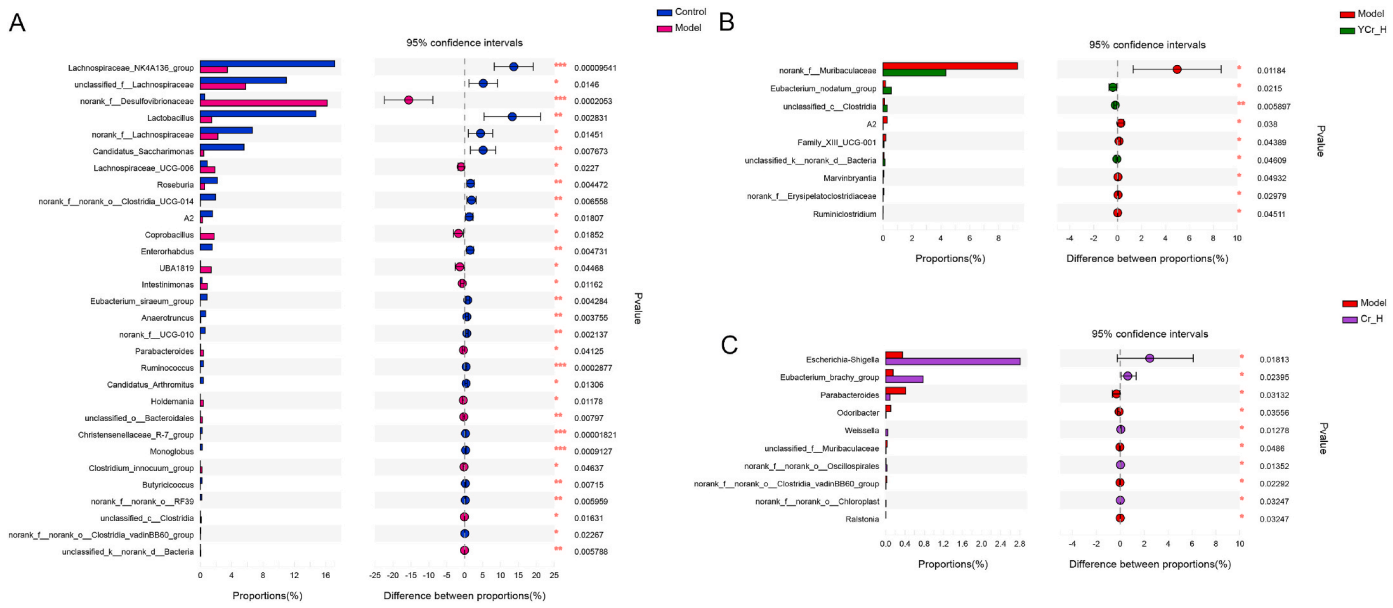

Fig. 6. Extended error bar plot comparing the differences in the mean proportions of significantly altered genera and the difference in the proportions of the means. The differences between experimental groups were determined using a Welsh's *t*-test, and the Benjamini-Hochberg procedure was used to control the false-discovery rate due to multiple testing. Corrected P values are shown at right. (A) Control *vs.* Model, (B) Model *vs.* YCr–H, and (C) Model *vs.* Cr–H.

(*Acsl1*) and bile salt export pump (*Bsep*) were remarkably up-regulated in mice fed with HFHFD, compared with the control group ($P < 0.05$). Oral administration of high-dose YCr significantly decreased mRNA expression of *Fatp-1*, *Ntcp*, *Dgat2*, *Acts1* and *Bsep*, but promoted mRNA expression of *Acox1*, *Cyp7a1*, *Akt*, *Glut4*, *FBPase*, *ApoE*, *Gk*, *Cpt*-1 and *Ldlr* in liver of mice fed with HFHFD ($P < 0.05$). These results indicated that both YCr and Cr interventions can effectively improve the abnormal expression of genes related to glucose and lipid metabolism in mice fed with HFHFD.

4. Discussion

It is well known that long-time high-energy diet consumption may result in hyperlipidemia, hyperglycemia and intestinal microbiota dysbiosis (Kopelman, 2000). Hyperlipidemia and hyperglycemia are important risk factor for the occurrence of other metabolic diseases, such as type 2 diabetes and arteriosclerosis, and have become public health challenges (Park et al., 2022). Previous study revealed that the serum Cr levels in patients with diabetes mellitus differed significantly from those of the healthy controls (Kazi et al., 2008). Dietary chromium (III) supplementation increases the insulin sensitivity and fasting glucose tolerance, thereby reducing the risk of hyperglycemia and atherosclerotic complications. Compared with inorganic chromium, the dietary intervention of organic chromium can reduce the toxic and side effects of inorganic chromium and reduce the direct stimulation to the gastrointestinal tract. In this study, after eight weeks of high-energy diet intervention, abnormal increase of body weight and liver index, dyslipidemia and liver lipid metabolism disorder were observed in the mice. However, both YCr intervention and Cr intervention can effectively inhibit the abnormal weight gain of HFHFD-fed mice and prevent the excessive accumulation of blood lipids. In comparison to inorganic chromium (Cr), YCr intervention has an advantage at enhancing fasting glucose tolerance, reducing serum TC, hepatic TG and hepatic glycogen levels, suggesting that YCr appeared to be more effective than inorganic chromium (Cr) in improving glucose and lipid metabolism in mice fed with HFHFD. It is well known that serum lipid level can directly reflect lipid metabolism status in the body. Previous study had shown that obese mice have higher serum TC, TG and LDL-C levels, but lower serum HDL-C levels, which is consistent with the serum results of our study (Xu et al., 2022). Higher levels of blood glucose, serum TC and TG may promote the occurrence and development of atherosclerosis (Guo et al., 2018; Fang et al., 2021). Serum LDL-C overload is one of the main factors leading to lipid metabolism disorder, which further induces apoptosis and inflammatory response (Li et al., 2017). As a beneficial apolipoprotein, HDL-C is considered to accelerate the degradation and metabolism of cholesterol (Liu et al., 2022). Interestingly, our results also showed that YCr supplementation can effectively inhibit the abnormal increases of fasting blood glucose levels caused by HFHFD, suggesting that YCr may help to prevent hyperglycemia. Cholesterol in the liver can be further converted into primary bile acids (BAs), which are stored in the gallbladder and conjugated with glycine or taurine, and released into the intestine in time to emulsify lipids. Most of the BAs can be reabsorbed by the small intestine, enter the liver and be recycled, while the remaining BAs are excreted through feces (Mullish et al., 2018). Interestingly, primary BAs can be transformed into secondary BAs through the metabolism of specific bacterial in the intestine. In this study, YCr supplementation efficiently reduced the accumulation of cholesterol and triglycerides in liver, and promoted the fecal excretion of BAs. Therefore, the ameliorative effects of YCr on lipid metabolism disorders is probably achieved by regulating intestinal microbiota composition, and thus promoting the transformation and fecal excretion of BAs.

Emerging evidences have revealed that intestinal microbiota may be a possible therapeutic or preventive candidate for hyperglycemia, dyslipidemia, pre-diabetes and NAFLD (Lupori et al., 2022). It was previously reported that high-energy diet-feeding may lead to significant reduce of the relative abundance of beneficial microbial phylotypes in intestinal tract, including *Lactobacillus*, *Bifidobacterium*, *Butyricicoccus* and *Akkermansia* (Guo et al., 2018). Our results showed that high-energy diet consumption significantly increased the proportion of harmful bacterial phylotypes such as *Holdemania* and *Coprobacillus*, but significantly decreased the relative abundance of beneficial bacterial phylotypes such as *Lachnospiraceae*_NK4A136_group, *Butyricicoccus*, *Roseburia*, *Ruminococcus* and *Clostridia*. *Holdemania* is a member of the Erysipelotrichaceae family, and its abundance is significantly positively correlated with the severity of lipid metabolism disorder (Zhao et al., 2021b). Previous report also showed that high abundance of *Holdemania* in the gut contributes to the induction of inflammatory responses (Jang

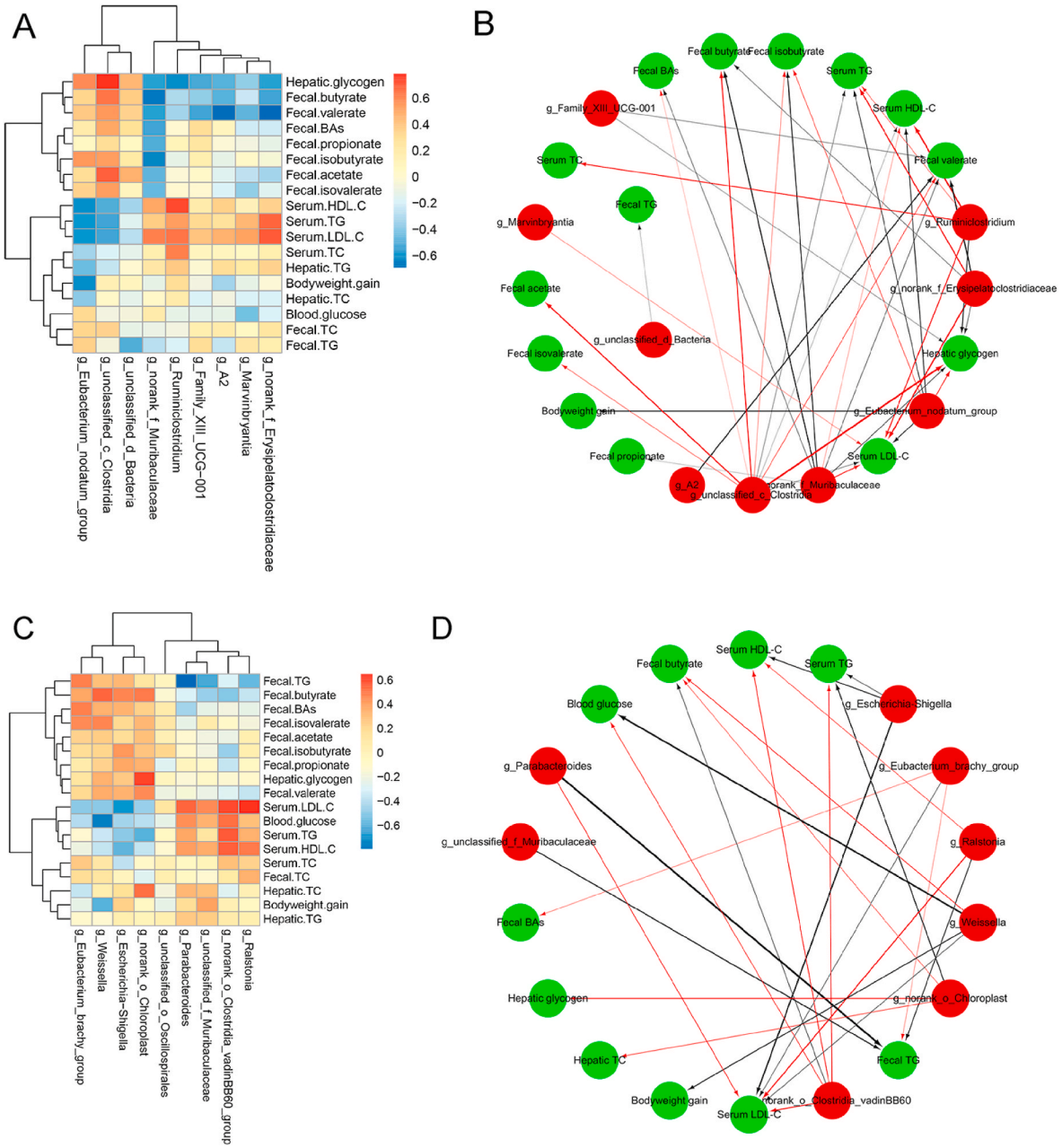

Fig. 7. Spearman's correlation of the key intestinal microbial phylotypes with biochemical parameters. Heatmap (A) and network (B) of correlation between the biochemical parameters and the significant alterative microbial phylotypes in HFD-fed mice with YCr intervention; Heatmap (C) and network (D) of correlation between the biochemical parameters and the significant alterative microbial phylotypes in HFD-fed mice with Cr intervention. The line width and color (red and black represented to positive and negative, respectively) are represented the correlation strength. (For interpretation of the references to color in this figure legend, the reader is referred to the Web version of this article.)

et al., 2020). The abundance of *Coprobacillus* in the intestine has been reported to be positively correlated with the serum levels of TC, TG and LDL-C, suggesting that the presence of high abundance of *Coprobacillus* may increase the occurrence of hyperlipidemia (Zhao et al., 2021b). These results showed that long-time consumption of high-fat diet impair the glucolipid metabolism and accelerate the inflammatory cytokines secretion by destroying the intestinal microbiota balance. Interestingly, 16S rRNA amplicon sequencing showed that YCr supplementation was beneficial to ameliorating the disturbance of intestinal microbiota by increasing the proportion of *Clostridia*, *Eubacterium_nodatum_*group, but reducing the proportion of *Muribaculaceae*, A2, Family_XIII_UCG-001, *Marvinbryantia* and *Erysipelatoclostridiaceae*. As a kind of symbiotic bacterium in the intestine, the abundance of *Clostridia* was reported to be negatively correlated with the incidence rate of obesity and metabolic syndrome (Ussar et al., 2016). A higher proportion of *Clostridia* in the intestinal tract can inhibit the uptake of long-chain fatty acids by inhibiting the expression of *CD36* in the liver, which is conducive to reducing the absorption of fatty acids and weight loss (Petersen et al., 2019). In addition, *Clostridia* has beneficial health effects in the intestinal tract, such as suppressing inflammatory responses and inducing regulatory T cell differentiation and accumulation (Atarashi et al., 2011). As a mesophilic anaerobic cellulose decomposing bacterium, *Eubacterium_nodatum_*group is generally considered to be one of the SCFAs producing bacteria in the intestine, which is involved in improving lipid metabolism, controlling energy intake, elevating the ability of the immune system and anti-inflammatory response. In this

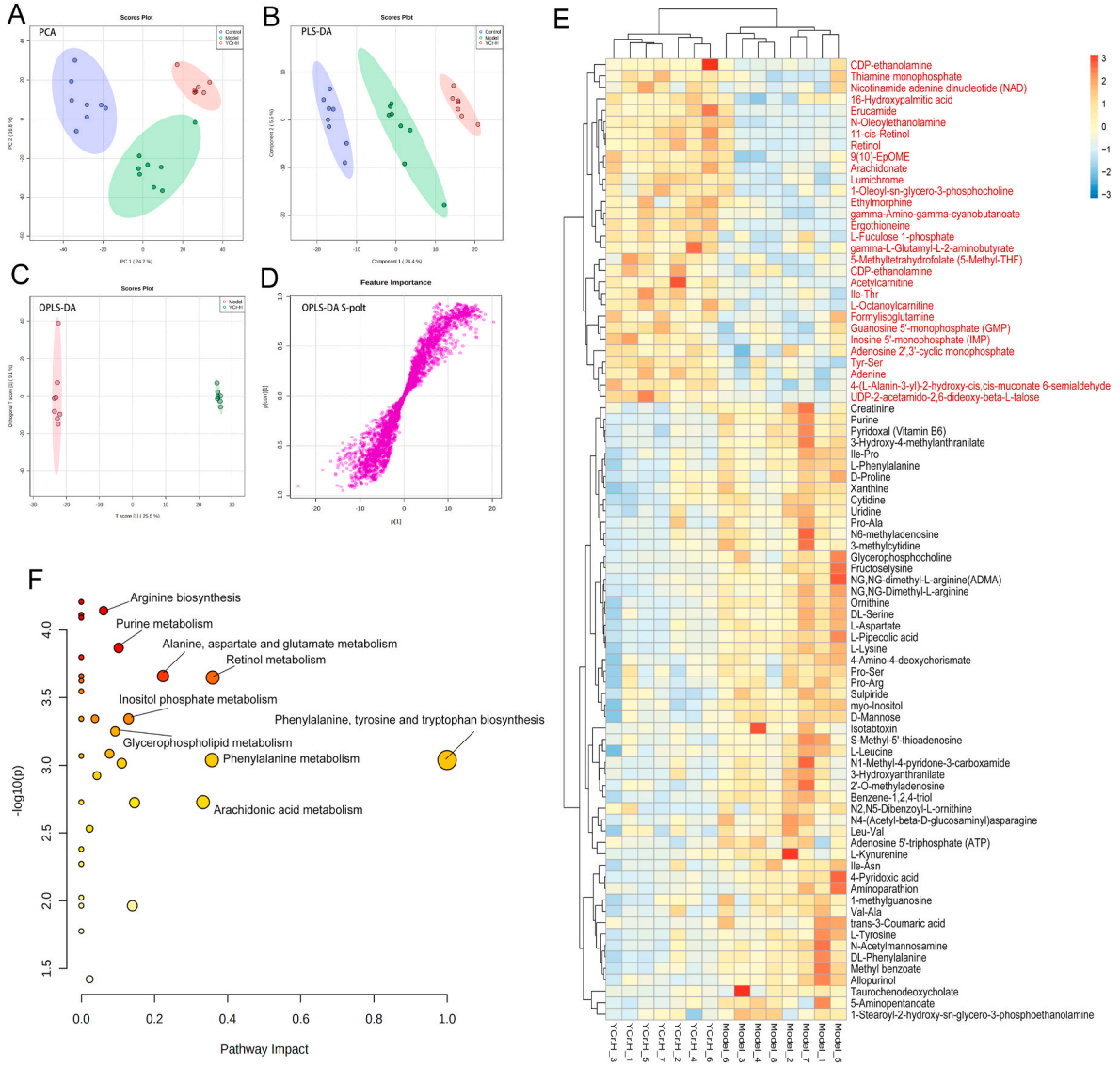

Fig. 8. Liver metabolomic profiling by UPLC-QTOF MS in the positive-ion mode (ESI+). (A) PCA score plot of the three groups (control, model and YCr–H groups), (B) PLS-DA score plot of the control, model and YCr–H groups, (C) OPLS-DA score plot of the model group and YCr group, (D) S-loading plot according to the OPLS-DA analysis of the YCr–H and model groups, (E) Differential metabolites clustering heatmap (VIP value > 1.0, $P < 0.05$) between the Model and YCr–H groups; (F) Metabolic pathway analysis based on significantly differential metabolites.

study, we found that the proportion of *Eubacterium_nodatum_*group was positively correlated with the fecal levels of butyrate, valerate, propionate, isobutyrate and acetate, which further indicated that *Eubacterium_nodatum_*group might be a potential producer of intestinal SCFAs. It was previously reported that *Eubacterium_nodatum_*group may be associated with glucose and lipid metabolism, and the increase of its relative abundance may contribute to the improvement of type 2 diabetes (Xiao et al., 2020). *Muribaculaceae*, which was significantly down-regulated by YCr intervention, was previously reported to cause lipid metabolism disorders by increasing host intake of high energy (Ye et al., 2021). It was previously reported that high fat diet may increase the proportion of the pathogenic bacterium Erysipelotrichaceae in mice (Chen et al., 2018), which has been reported to be related to obesity, colorectal cancer, etc (Bailén et al., 2020). Interestingly, Cr intervention significantly increased the proportion of *Weissella* in the intestinal tract of HFHFD-fed mice. The lactate-producing genus *Weissella* has been reported to contribute positively to cholesterol reduction and weight loss, possibly due to its ability to produce large amounts of bacteriocin and exopolysaccharides, which has been proven to inhibit the proliferation of pathogenic bacteria and regulate host immunity (Kavitake et al., 2020; Fhoula et al., 2018). In conclusion, both YCr and Cr interventions can alter the composition of intestinal flora, which may have a potential contribution to the maintenance of glucose and lipid homeostasis. Of course, the specific role of intestinal microbes in YCr and Cr intervention in improving hyperglycemia and hyperlipidemia remains to be verified through fecal bacteria transplantation or germ-free mouse experiments in our further study.

Liver is the most important organ that plays a vital role for regulating and maintaining the homeostasis of glucose and lipid metabolism *in vivo*. Long-time consumption of high-energy diet accelerates the accumulation of lipid in the liver, which increase the burden of liver function. In this study, liver metabolomics was used to further explore the protective mechanism of YCr on hyperglycemia and hyperlipidemia. Results showed that dietary intervention with YCr significantly increased the levels of retinol, arachidonate, ergothioneine, acetylcarnitine, but reduced the levels of 4-pyridoxic acid, kynurenine and taurochenodeoxycholate in liver. As an essential fat-soluble micronutrient, retinol was reported to be negatively correlated with plasma cholesterol

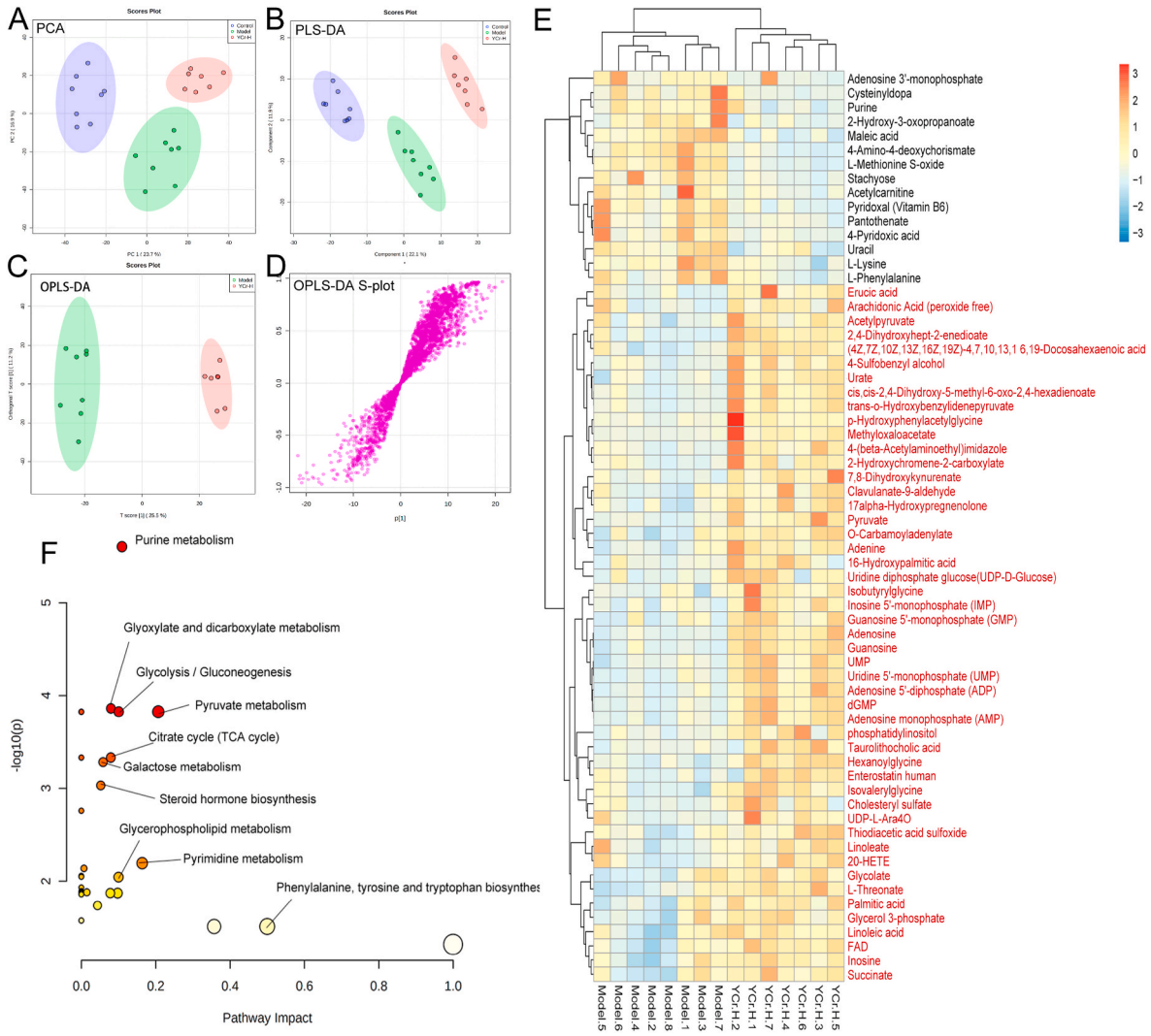

Fig. 9. Liver metabolomic profiling by UPLC-QTOF MS in the negative-ion mode (ESI-). (A) PCA score plot of the three groups (control, model and YCr–H groups), (B) PLS-DA score plot of the control, model and YCr–H groups, (C) OPLS-DA score plot of the model group and YCr group, (D) S-loading plot according to the OPLS-DA analysis of the YCr–H and model groups, (E) Differential metabolites clustering heatmap (VIP value > 1.0, $P < 0.05$) between the Model and YCr–H groups; (F) Metabolic pathway analysis based on significantly differential metabolites.

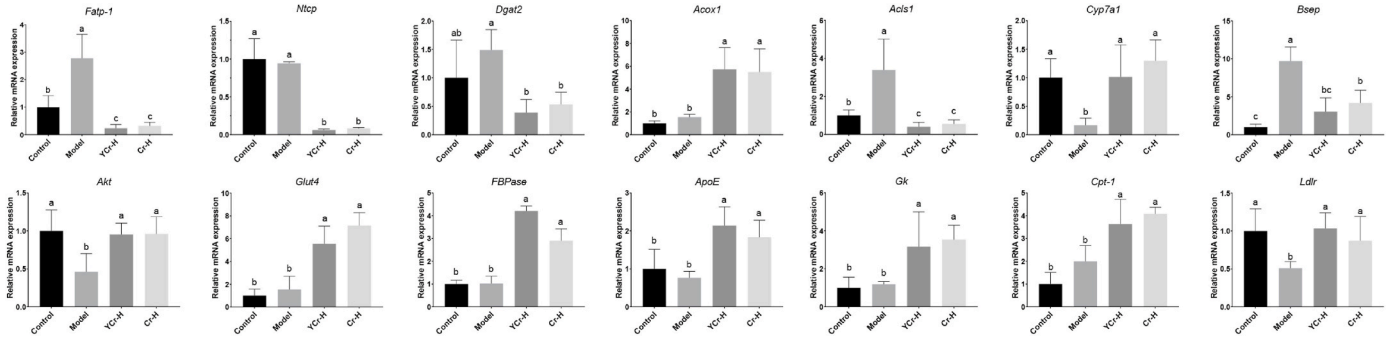

Fig. 10. Effects of high-dose YCr intervention on mRNA levels of genes responsible for glucose and lipid metabolism in mice fed with a high-fructose and high-fat diet. Columns with different letters are statistical significance by Duncan's multiple range test ($P < 0.05$).

level, inhibiting lipid overaccumulation in mammals, and thereby is beneficial for reducing the occurrence of atherosclerosis (Zhou et al., 2020). In addition, retinol can be metabolized into retinoic acid in the liver, which further stimulates liver lipolysis and reduces triglyceride level (Wolf, 2010). The presence of arachidonic acid can promote the biosynthesis of long-chain unsaturated fatty acids, and then reduce the concentration of free fatty acids in liver (Hatziantoniou et al., 2004). Ergothioneine is regarded as a powerful scavenger of various reactive oxygen species (ROS), which may avoid the damage of cellular constituents and maintain the function of mitochondrion (Kushairi et al.,

2020). In addition, acetylcarnitine protects the liver from oxidative stress by elevating the activities of glutathione peroxidase (Salman et al., 2016). 4-Pyridoxic acids, formed from pyridoxal by aldehyde oxidase, is a strong positive predictor of vascular risk score (Obeid et al., 2019). Kynurenine is a direct precursor of kynurenic acid, was reported to be obviously increased in tumor-bearing mice (Haggerty and Sullivan, 1960). As a potential marker of liver injury (Tian et al., 2017), taurochenodeoxycholate is synthesized in gut through microbial fermentation and is closely associated with glycolysis and fatty acid biosynthesis (Wang et al., 2018). It was previously reported that a high-cholesterol diet increased the hepatic level of taurochenodeoxycholate involved in primary bile acids biosynthesis (Li et al., 2020), which is in good agreement with the data of our study. In addition, taurochenodeoxycholate could reduce the expression of *Fxr* (Huang et al., 2019; Zhao et al., 2021a). Activation of *Fxr* could alleviate NAFLD by lowering hepatic and plasma lipid levels, reducing inflammation, and increasing insulin sensitivity (Clifford et al., 2021; Lin et al., 2021).

To clarify the preventive mechanism of YCr intervention on hyperlipidemia and hyperglycemia, mRNA levels of genes closely related to glucose and lipid metabolism in liver were detected by RT-qPCR. As a key metabolic enzyme in cholesterol metabolism, the activation of *Cyp7a1* promotes the conversion of cholesterol to BAs and the excretion of BAs into the intestine, which is further transformed into secondary BAs by intestinal microbial metabolism (Ghaffarzadegan et al., 2019). However, more than 90% of secondary BAs are re-absorbed into the liver to form bile acid cycle under the regulation of *Ntcp* and *Bsep*. YCr intervention promoted the expression of *Cyp7a1*, suppressed the expression of *Ntcp* and *Bsep*, and then promote the conversion of excess cholesterol in the liver into bile acids and excrete them with feces. Besides, this study showed that YCr intervention increased the mRNA expression levels of *ApoE*, *Ldlr*, *Acox1* and *Cpt*-1 genes, but inhibited the expressions of *Fatp* and *Acls1* genes. *ApoE* gene plays an important role in maintaining and regulating serum lipid homeostasis, especially serum HDL-C and VLDL-C concentrations. As a cell-surface glycoprotein, *Ldlr* is mainly responsible for regulating blood and intracellular cholesterol homeostasis, and deficiency of the *Ldlr* gene may significantly increase the risk of coronary heart disease (Awan et al., 2011). *Acox1* gene has been shown to be involved in the activation of fatty acid β-oxidation, and higher expression of *Acox1* is beneficial to the reduction of fatty acid storage (Guo et al., 2020b). As a key rate-limiting enzyme of mitochondrial fatty acid oxidation, the reduced mRNA expression of *Cpt*-1 gene leads to the restriction of fatty acid β-oxidation and the excessive accumulation of fatty acids in the liver. It has been proved that high-calorie diet may activate the expression of *Fatp* and *Acls1*, leading to the excessive synthesis of fatty acids in liver. *Acls1* is an important enzyme that control the synthesis of complex chain fatty acids by promoting the conversion of acetyl-CoA to malonyl-CoA, thereby disrupting energy homeostasis (Sim et al., 2015). It is well known that inorganic chromium (III) supplements significantly alleviate the diabetic-like symptoms because chromium (III) is an essential trace component of glucose tolerance factor (Refat et al., 2017). As a major regulator to activate the glucose metabolism (He et al., 2020), *Akt* activation potentiates glucose uptake by inducing *Glut4* translocation to the plasma membrane, thereby facilitating glucose transport into cells and normalizing the blood glucose levels (Huang et al., 2021). As a member of the insulin-responding glucose transporters, *Glut4* gene is mainly involved in glucose uptake in cells. Our study showed that the transcription level of *Glut4* gene in liver of mice of the YCr groups was significantly higher than that of the model group, indicating that oral administration of YCr can maintain glucose homeostasis *in vivo* by enhancing glucose entry into cells. In addition, high expression of *Gk* can control blood glucose through accelerating insulin secretion and glycogen synthesis, which is beneficial for further reduced the blood glucose. *FBPase* is a key rate-limiting enzyme, which directly intervene glycogenolysis, glycolysis, and the tricarboxylic acid cycle (Xu et al., 2020).

5. Conclusions

In present study, the preventive effects of YCr intervention and Cr intervention on hyperlipidemia and hyperglycemia were explored from intestinal microbiomics and liver metabolomics insights. Results showed that both of YCr and Cr interventions remarkably improved hyperglycemia, hyperlipidemia and intestinal microbial imbalance in mice induced by HFHFD-feeding, but the improvement effects of YCr intervention was better than those of Cr intervention. Liver metabolomics and RT-qPCR analysis revealed that YCr intervention regulated liver metabonomic profile and liver mRNA levels of key genes associated with glucose and lipid metabolism. This study provides useful information for excavating functional foods to prevent hyperlipidemia and hyperglycemia. In future study, the effects of YCr on hyperlipidemia and hyperglycemia also need to be verified through clinical population trials.

CRediT authorship contribution statement

Mei-Ting Wang: Methodology, Investigation, Writing – original draft, Validation. **Wei-Ling Guo:** Investigation, Writing – original draft. **Zi-Yi Yang:** Investigation, Writing – original draft. **Feng Chen:** Investigation, Software. **Tian-Tian Lin:** Data curation, Software. **Wen-Long Li:** Software, Writing – review & editing. **Xu-Cong Lv:** Funding acquisition, Writing – review & editing, Supervision, Conceptualization, Project administration. **Ping-Fan Rao:** Supervision, Conceptualization. **Lian-Zhong Ai:** Supervision, Conceptualization. **Li Ni:** Supervision, Conceptualization, Writing – review & editing.

Declaration of competing interest

The authors declare that they have no known competing financial interests or personal relationships that could have appeared to influence the work reported in this paper.

Acknowledgments

This work was supported by funding from Outstanding Talent of "Qishan Scholar" of Fuzhou University (GXRC21049). Metabolomics analysis was assisted by Biotree Biotech Co., Ltd. (Shanghai, China).

Appendix A. Supplementary data

Supplementary data to this article can be found online at https://doi.org/10.1016/j.crfs.2022.08.015.

References

Atarashi, K., Tanoue, T., Shima, T., Imaoka, A., Kuwahara, T., Momose, Y., Cheng, G., Yamasaki, S., Saito, T., Ohba, Y., Taniguchi, T., Takeda, K., Hori, S., Ivanov II, Umesaki, Y., Itoh, K., Honda, K., 2011. Induction of colonic regulatory T cells by indigenous Clostridium species. Science (New York, N.Y.) 331, 337–341. https://doi.org/10.1126/science.1198469.

Awan, Z., Denis, M., Bailey, D., Giaid, A., Prat, A., Goltzman, D., Seidah, N.G., Genest, J., 2011. The LDLR deficient mouse as a model for aortic calcification and quantification by micro-computed tomography. Atherosclerosis 219, 455–462. https://doi.org/10.1016/j.atherosclerosis.2011.08.035.

Bailén, M., Bressa, C., Martínez-López, S., González-Soltero, R., Montalvo Lominchar, M. G., San Juan, C., Larrosa, M., 2020. Microbiota features associated with a high-fat/low-fiber diet in healthy adults. Front. Nutr. 7, 1–13. https://doi.org/10.3389/fnut.2020.583608.

Çakır, I., Hadley, C.K., Pan, P.L., Bagchi, R.A., Ghamari-Langroudi, M., Porter, D.T., Wang, Q., Litt, M.J., Jana, S., Hagen, S., Lee, P., White, A., Lin, J.D., McKinsey, T.A., Cone, R.D., 2022. Histone deacetylase 6 inhibition restores leptin sensitivity and reduces obesity. Nat. Metab. 4, 44–59. https://doi.org/10.1038/s42255-021-00515-3.

Canfora, E.E., Jocken, J.W., Blaak, E.E., 2015. Short-chain fatty acids in control of body weight and insulin sensitivity. Nat. Rev. Endocrinol. 11, 577–591. https://doi.org/10.1038/nrendo.2015.128.

Chalasani, N., Younossi, Z., Lavine, J.E., Charlton, M., Cusi, K., Rinella, M., Harrison, S. A., Brunt, E.M., Sanyal, A.J., 2018. The diagnosis and management of nonalcoholic fatty liver disease: practice guidance from the American Association for the Study of Liver Diseases. Hepatology 67, 328–357. https://doi.org/10.1002/hep.29367.

Chen, G., Xie, M., Wan, P., Chen, D., Dai, Z., Ye, H., et al., 2018. Fuzhuan brick tea polysaccharides attenuate metabolic syndrome in high-fat diet induced mice in association with modulation in the gut microbiota. J. Agric. Food Chem. 66 (11), 2783–2795. https://doi.org/10.1021/acs.jafc.8b00296.

Chen, H., Yang, H., Deng, J., Fan, D., 2021. Ginsenoside Rk3 ameliorates obesity-induced colitis by regulating of intestinal flora and the TLR4/NF-κB signaling pathway in C57bl/6 mice. J. Agric. Food Chem. 69, 3082–3093. https://doi.org/10.1021/acs.jafc.0c07805.

Chen, M., Guo, W.-L., Li, Q.-Y., Xu, J.-X., Cao, Y.-J., Liu, B., Yu, X.-D., Rao, P.-F., Ni, L., Lv, X.-C., 2020. The protective mechanism of *Lactobacillus plantarum* FZU3013 against non-alcoholic fatty liver associated with hyperlipidemia in mice fed a high-fat diet. Food Funct. 11, 3316–3331. https://doi.org/10.1039/c9fo03003d.

Clifford, B.L., Sedgeman, L.R., Williams, K.J., Morand, P., Cheng, A., Jarrett, K.E., Chan, A.P., Brearley-Sholto, M.C., Wahlström, A., Ashby, J.W., Barshop, W., Wohlschlegel, J., Calkin, A.C., Liu, Y., Thorell, A., Meikle, P.J., Drew, B.G., Mack, J. J., Marschall, H.U., Tarling, E.J., Edwards, P.A., de Aguiar Vallim, T.Q., 2021. FXR activation protects against NAFLD via bile-acid-dependent reductions in lipid absorption. Cell Metabol. 33, 1671–1684. https://doi.org/10.1016/j.cmet.2021.06.012.

Fang, D., Wang, D., Ma, G., Ji, Y., Zheng, H., Chen, H., Zhao, M., Hu, Q., Zhao, L., 2021. *Auricularia polytricha* noodles prevent hyperlipemia and modulate gut microbiota in high-fat diet fed mice. Food Sci. Hum. Wellness 10, 431–441. https://doi.org/10.1016/j.fshw.2021.04.005.

Fhoula, I., Rehaiem, A., Najjari, A., Usai, D., Boudabous, A., Sechi, L.A., Hadda-Imene, O., 2018. Functional probiotic assessment and in vivo cholesterol-lowering efficacy of *Weissella* sp. associated with arid lands living-hosts. BioMed Res. Int., 1654151 https://doi.org/10.1155/2018/1654151, 2018.

Ghaffarzadegan, T., Essén, S., Verbrugghe, P., Marungruang, N., Hållenius, F.F., Nyman, M., Sandahl, M., 2019. Determination of free and conjugated bile acids in serum of Apoe(−/−) mice fed different lingonberry fractions by UHPLC-MS. Sci. Rep. 9, 3800. https://doi.org/10.1038/s41598-019-40272-8.

Gujjala, S., Putakala, M., Ramaswamy, R., Desireddy, S., 2016. Preventive effect of Caralluma fimbriata vs. Metformin against high-fat diet-induced alterations in lipid metabolism in Wistar rats. Biomed. Pharmacother. 84, 215–223. https://doi.org/10.1016/j.biopha.2016.09.029.

Guo, W.L., Chen, M., Pan, W.L., Zhang, Q., Xu, J.X., Lin, Y.C., Li, L., Liu, B., Bai, W.D., Zhang, Y.Y., Ni, L., Rao, P.F., Lv, X.C., 2020a. Hypoglycemic and hypolipidemic mechanism of organic chromium derived from chelation of *Grifola frondosa* polysaccharide-chromium (III) and its modulation of intestinal microflora in high fat-diet and STZ-induced diabetic mice. Int. J. Biol. Macromol. 145, 1208–1218. https://doi.org/10.1016/j.ijbiomac.2019.09.206.

Guo, W.L., Deng, J.C., Pan, Y.Y., Xu, J.X., Hong, J.L., Shi, F.F., Liu, G.L., Qian, M., Bai, W. D., Zhang, W., Liu, B., Zhang, Y.Y., Luo, P.-J., Ni, L., Rao, P.F., Lv, X.C., 2020b. Hypoglycemic and hypolipidemic activities of *Grifola frondosa* polysaccharides and their relationships with the modulation of intestinal microflora in diabetic mice induced by high-fat diet and streptozotocin. Int. J. Biol. Macromol. 153, 1231–1240. https://doi.org/10.1016/j.ijbiomac.2019.10.253.

Guo, W.L., Guo, J.B., Liu, B.Y., Lu, J.Q., Chen, M., Liu, B., Bai, W.D., Rao, P.F., Ni, L., Lv, X.C., 2020c. Ganoderic acid A from *Ganoderma lucidum* ameliorates lipid metabolism and alters gut microbiota composition in hyperlipidemic mice fed a high-fat diet. Food Funct. 11, 6818–6833. https://doi.org/10.1039/d0fo00436g.

Guo, W.L., Pan, Y.Y., Li, L., Li, T.T., Liu, B., Lv, X.C., 2018. Ethanol extract of *Ganoderma lucidum* ameliorates lipid metabolic disorders and modulates the gut microbiota composition in high-fat diet fed rats. Food Funct. 9, 3419–3431. https://doi.org/10.1039/c8fo00836a.

Haggerty, J.F., Sullivan, M.X., 1960. Kynurenine accumulation in tumor-bearing mice. Acta Unio Int. Contra Cancrum 16, 1068–1073. PMID: 14398815.

Hatziantoniou, S., Giamarellos-Bourboulis, E.J., Skiathitis, S., Demetzos, C., Donta, I., Papaioannou, G.T., Dionyssiou-Asteriou, A., Karayannacos, P.E., Giamarellou, H., 2004. Rapid alterations of serum fatty acids with the intravenous administration of an arachidonate solution. Prostaglandins Leukot. Essent. Fatty Acids 70, 465–468. https://doi.org/10.1016/j.plefa.2003.09.002.

Hayat, K., Bodinga, B.M., Han, D., Yang, X., Sun, Q., Aleya, L., Abdel-Daim, M.M., Yang, X., 2020. Effects of dietary inclusion of chromium propionate on growth performance, intestinal health, immune response and nutrient transporter gene expression in broilers. Sci. Total Environ. 705, 135869 https://doi.org/10.1016/j.scitotenv.2019.135869.

He, C.J., Ma, L.Q., Iqbal, M.S., Huang, X.J., Li, J., Yang, G.Z., Ihsan, A., 2020. Veratrilla baillonii Franch exerts anti-diabetic activity and improves liver injury through IRS/PI3K/AKT signaling pathways in type 2 diabetic db/db mice. J. Funct.Foods 75, 104204. https://doi.org/10.1016/j.jff.2020.104204.

Hou, Y.B., Hou, Y., Yao, L., Chen, S., Fan, J.H., Qian, L.C., 2019. Effects of chromium yeast, tributyrin and bile acid on growth performance, digestion and metabolism of *Channa argus*. Aquacult. Res. 50 (3), 836–846. https://doi.org/10.1111/are.13954.

Hosseinzadeh, P., D Jazayery, A., Mostafavi, S.A., Javanbakht, M.H., Derakhshanian, H., Rahimiforoushani, A., et al., 2013. Brewer's yeast improves blood pressure in type 2 diabetes mellitus. Iran. J. Public Health 42 (6), 602.

Huang, F., Zheng, X., Ma, X., Jiang, R., Zhou, W., Zhou, S., Zhang, Y., Lei, S., Wang, S., Kuang, J., Han, X., Wei, M., You, Y., Li, M., Li, Y., Liang, D., Liu, J., Chen, T., Yan, C., Wei, R., Rajani, C., Shen, C., Xie, G., Bian, Z., Li, H., Zhao, A., Jia, W., 2019. Theabrownin from Pu-erh tea attenuates hypercholesterolemia via modulation of gut microbiota and bile acid metabolism. Nat. Commun. 10, 4971–4987. https://doi.org/10.1038/s41467-019-12896-x.

Huang, Y., Zhou, T., Zhang, Y., Huang, H., Ma, Y., Wu, C., Wang, Q., Lin, Q., Yang, X., Pang, K., 2021. Antidiabetic activity of a Flavonoid-Rich extract from flowers of Wisteria sinensis in type 2 diabetic mice via activation of the IRS-1/PI3K/Akt/GLUT4 pathway. J. Funct.Foods 77, 104338. https://doi.org/10.1016/j.jff.2020.104338.

Jang, J.H., Yeom, M.J., Ahn, S., Oh, J.Y., Ji, S., Kim, T.H., Park, H.J., 2020. Acupuncture inhibits neuroinflammation and gut microbial dysbiosis in a mouse model of Parkinson's disease. Brain Behav. Immun. 89, 641–655. https://doi.org/10.1016/j.bbi.2020.08.015.

D.J.J.o.F.F Jaroslav, A., Kralovec, Michael, A., Potvin, Jeffrey, H., 2009. Chromium(III)–docosahexaenoic acid complex: synthesis and characterization. J. Funct.Foods 1 (3), 291–297. https://doi.org/10.1016/j.jff.2009.06.001.

Kavitake, D., Devi, P.B., Shetty, P.H., 2020. Overview of exopolysaccharides produced by Weissella genus-A review. Int. J. Biol. Macromol. 164, 2964–2973. https://doi.org/10.1016/j.ijbiomac.2020.08.185.

Kazi, T.G., Afridi, H.I., Kazi, N., Jamali, M.K., Arain, M.B., Jalbani, N., Kandhro, G.A., 2008. Copper, chromium, manganese, iron, nickel, and zinc levels in biological samples of diabetes mellitus patients. Biol. Trace Elem. Res. 122 (1), 1–18. https://doi.org/10.1007/s12011-007-8062-y.

Kopelman, P.G., 2000. Obesity as a medical problem. Nature 404, 635–643. https://doi.org/10.1038/35007508.

Król, E., Krejpcio, Z., Byks, H., Bogdański, P., Pupek-Musialik, D., 2011. Effects of chromium brewer's yeast supplementation on body mass, blood carbohydrates, and lipids and minerals in type 2 diabetic patients. Biol. Trace Elem. Res. 143 (2), 726–737. https://doi.org/10.1007/s12011-010-8917-5.

Kushairi, N., Phan, C.W., Sabaratnam, V., Naidu, M., David, P., 2020. Dietary amino acid ergothioneine protects HT22 hippocampal neurons against H_2O_2-induced neurotoxicity via antioxidative mechanism. Pharma. Nutr. 13, 100214 https://doi.org/10.1016/j.phanu.2020.100214.

Li, J., Zhao, F., Wang, Y., Chen, J., Tao, J., Tian, G., Wu, S., Liu, W., Cui, Q., Geng, B., Zhang, W., Weldon, R., Auguste, K., Yang, L., Liu, X., Chen, L., Yang, X., Zhu, B., Cai, J., 2017. Gut microbiota dysbiosis contributes to the development of hypertension. Microbiome 5, 14. https://doi.org/10.1186/s40168-016-0222-x.

Li, L., Xu, J.X., Cao, Y.J., Lin, Y.C., Guo, W.L., Liu, J.Y., Bai, W.D., Zhang, Y.Y., Ni, L., Liu, B., Rao, P.F., Lv, X.C., 2019. Preparation of *Ganoderma lucidum* polysaccharide-chromium (III) complex and its hypoglycemic and hypolipidemic activities in high-fat and high-fructose diet-induced pre-diabetic mice. Int. J. Biol. Macromol. 140, 782–793. https://doi.org/10.1016/j.ijbiomac.2019.08.072.

Li, X., Xiao, Y., Song, L., Huang, Y., Chu, Q., Zhu, S., Lu, S., Hou, L., Li, Z., Li, J., Xu, J., Ren, Z., 2020. Effect of Lactobacillus plantarum HT121 on serum lipid profile, gut microbiota, and liver transcriptome and metabolomics in a high-cholesterol diet-induced hypercholesterolemia rat model. Nutrition 79–80, 110966. https://doi.org/10.1016/j.nut.2020.110966.

Lin, Y., Chen, H., Cao, Y., Zhang, Y., Li, W., Guo, W., Lv, X., Rao, P., Ni, L., Liu, P., 2021. Auricularia auricula melanin protects against alcoholic liver injury and modulates intestinal microbiota composition in mice exposed to alcohol intake. Foods 10, 2436. https://doi.org/10.3390/foods10102436.

Liu, Z., Zhang, Y., Ai, C., Tian, W., Wen, C., Song, S., Zhu, B., 2022. An acidic polysaccharide from Patinopecten yessoensis skirt prevents obesity and improves gut microbiota and metabolism of mice induced by high-fat diet. Food Res. Int. 154, 110980 https://doi.org/10.1016/j.foodres.2022.110980.

Lupori, L., Cornuti, S., Mazziotti, R., Borghi, E., Ottaviano, E., Cas, M.D., Sagona, G., Pizzorusso, T., Tognini, P., 2022. The gut microbiota of environmentally enriched mice regulates visual cortical plasticity. Cell Rep. 38, 110212 https://doi.org/10.1016/j.celrep.2021.110212.

Lv, X.C., Chen, M., Huang, Z.R., Guo, W.L., Ai, L.Z., Bai, W.D., Yu, X.D., Liu, Y.L., Rao, P. F., Ni, L., 2021. Potential mechanisms underlying the ameliorative effect of *Lactobacillus paracasei* FZU103 on the lipid metabolism in hyperlipidemic mice fed a high-fat diet. Food Res. Int. 139, 109956 https://doi.org/10.1016/j.foodres.2020.109956.

Maares, M., Keil, C., Pallasdies, L., Schmacht, M., Senz, M., Nissen, J., Kieserling, H., Drusch, S., Haase, H., 2022. Zinc availability from zinc-enriched yeast studied with an in vitro digestion/Caco-2 cell culture model. J. Trace Elem. Med. Biol. 71, 126934 https://doi.org/10.1016/j.jtemb.2022.126934.

Miyamoto, J., Igarashi, M., Watanabe, K., Karaki, S.-i., Mukouyama, H., Kishino, S., Li, X., Ichimura, A., Irie, J., Sugimoto, Y., Mizutani, T., Sugawara, T., Miki, T., Ogawa, J., Drucker, D.J., Arita, M., Itoh, H., Kimura, I., 2019. Gut microbiota confers host resistance to obesity by metabolizing dietary polyunsaturated fatty acids. Nat. Commun. 10, 4007. https://doi.org/10.1038/s41467-019-11978-0.

Mullish, B.H., Pechlivanis, A., Barker, G.F., Thursz, M.R., Marchesi, J.R., McDonald, J.A. K., 2018. Functional microbiomics: evaluation of gut microbiota-bile acid metabolism interactions in health and disease. Methods 149, 49–58. https://doi.org/10.1016/j.ymeth.2018.04.028.

Obeid, R., Geisel, J., Nix, W.A., 2019. 4-Pyridoxic Acid/Pyridoxine ratio in patients with type 2 diabetes is related to global cardiovascular risk scores. Diagnostics 9 (1), 28. https://doi.org/10.3390/diagnostics9010028.

Park, S.J., Kim, J.L., Park, M.R., Lee, J.W., Kim, O.K., Lee, J., 2022. Indian gooseberry and barley sprout mixture prevents obesity by regulating adipogenesis, lipogenesis, and lipolysis in C57BL/6J mice with high-fat diet-induced obesity. J. Funct.Foods 90, 104951. https://doi.org/10.1016/j.jff.2022.104951.

Petersen, C., Bell, R., Klag, K.A., Lee, S.H., Soto, R., Ghazaryan, A., Buhrke, K., Ekiz, H.A., Ost, K.S., Boudina, S., O'Connell, R.M., Cox, J.E., Villanueva, C.J., Stephens, W.Z., Round, J.L., 2019. T cell-mediated regulation of the microbiota protects against obesity. Science 365 (6451), eaat9351. https://doi.org/10.1126/science.aat9351.

Quievryn, G., Peterson, E., Messer, J., Zhitkovich, A., 2003. Genotoxicity and mutagenicity of chromium(VI)/ascorbate-generated DNA adducts in human and bacterial cells. Biochemistry 42, 1062–1070. https://doi.org/10.1021/bi0271547.

Refat, M.S., El-Megharbel, S.M., Hussien, M.A., Hamza, R.Z., Al-Omar, M.A., Naglah, A. M., Afifi, W.M., Kobeasy, M.I., 2017. Spectroscopic, structural characterizations and

antioxidant capacity of the chromium (III) niacinamide compound as a diabetes mellitus drug model. Spectrochim. Acta Mol. Biomol. Spectrosc. 173, 122–131. https://doi.org/10.1016/j.saa.2016.08.053.

Salman, A.A., Abdulrazaq, A., Saleh, A.B., Naif, O.A., Mahmoud, N.N., 2016. Prophylactic and therapeutic potential of acetyl-L-carnitine against acetaminophen-induced hepatotoxicity in mice. J. Biochem. Mol. Toxicol. 30, 5–11. https://doi.org/10.1002/jbt.21733.

Savva, C., Helguero, L.A., González-Granillo, M., Melo, T., Couto, D., Buyandelger, B., Gustafsson, S., Liu, J., Domingues, M.R., Li, X., Korach-André, M., 2022. Maternal high-fat diet programs white and brown adipose tissue lipidome and transcriptome in offspring in a sex- and tissue-dependent manner in mice. Int. J. Obes. 46, 831–842. https://doi.org/10.1038/s41366-021-01060-5.

Shan, Q., Ma, F.T., Jin, Y.H., Gao, D., Li, H.Y., Sun, P., 2020. Chromium yeast alleviates heat stress by improving antioxidant and immune function in Holstein mid-lactation dairy cows. Anim. Feed Sci. Technol. 269, 114635 https://doi.org/10.1016/j.anifeedsci.2020.114635.

Sim, M.O., Lee, H.I., Ham, J.R., Seo, K.I., Lee, M.K., 2015. Long-term supplementation of esculetin ameliorates hepatosteatosis and insulin resistance partly by activating AdipoR2–AMPK pathway in diet-induced obese mice. J. Funct.Foods 15, 160–171. https://doi.org/10.1016/j.jff.2015.03.014.

Sundaram, B., Aggarwal, A., Sandhir, R., 2013. Chromium picolinate attenuates hyperglycemia-induced oxidative stress in streptozotocin-induced diabetic rats. J. Trace Elem. Med. Biol. 27, 117–121. https://doi.org/10.1016/j.jtemb.2012.09.002.

Tian, J., Zhu, J., Yi, Y., Li, C., Zhang, Y., Zhao, Y., Pan, C., Xiang, S., Li, X., Li, G., Newman, J.W., Feng, X., Liu, J., Han, J., Wang, L., Gao, Y., La Frano, M.R., Liang, A., 2017. Dose-related liver injury of Geniposide associated with the alteration in bile acid synthesis and transportation. Sci. Rep. 7, 1–11. https://doi.org/10.1038/s41598-017-09131-2.

Ussar, S., Griffin, Nicholas W., Bezy, O., Fujisaka, S., Vienberg, S., Softic, S., Deng, L., Bry, L., Gordon, Jeffrey I., Kahn, C.R., 2016. Interactions between gut microbiota, host genetics and diet modulate the predisposition to obesity and metabolic syndrome. Cell Metabol. 23, 564–566. https://doi.org/10.1016/j.cmet.2015.07.007.

Wang, W., Zhao, J., Gui, W., Sun, D., Dai, H., Xiao, L., Chu, H., Du, F., Zhu, Q., Schnabl, B., Huang, K., Yang, L., Hou, X., 2018. Tauroursodeoxycholic acid inhibits intestinal inflammation and barrier disruption in mice with non-alcoholic fatty liver disease. Br. J. Pharmacol. 175, 469–484. https://doi.org/10.1111/bph.14095.

Wolf, G., 2010. Retinoic acid activation of peroxisome proliferation-activated receptor delta represses obesity and insulin resistance. Nutr. Rev. 68 (1), 67–70. https://doi.org/10.1111/j.1753-4887.2009.00261.x.

Xiao, S., Liu, C., Chen, M., Zou, J., Zhang, Z., Cui, X., Jiang, S., Shang, E., Qian, D., Duan, J., 2020. Scutellariae radix and coptidis rhizoma ameliorate glycolipid metabolism of type 2 diabetic rats by modulating gut microbiota and its metabolites. Appl. Microbiol. Biotechnol. 104, 303–317. https://doi.org/10.1007/s00253-019-10174-w.

Xu, M., Lv, C., Wang, H., Lu, Q., Ye, M., Zhu, X., Liu, R., 2022. Peanut skin extract ameliorates high-fat diet-induced atherosclerosis by regulating lipid metabolism, inflammation reaction and gut microbiota in ApoE$^{-/-}$ mice. Food Res. Int. 154, 111014 https://doi.org/10.1016/j.foodres.2022.111014.

Xu, Y.X., Huang, Y.Y., Song, R.R., Ren, Y.L., Chen, X., Zhang, C., Mao, F., Li, X.K., Zhu, J., Ni, S.S., Wan, J., Li, J., 2020. Development of disulfide-derived fructose-1,6-bisphosphatase (FBPase) covalent inhibitors for the treatment of type 2 diabetes. Eur. J. Med. Chem. 203, 112500 https://doi.org/10.1016/j.ejmech.2020.112500.

Ye, J., Zhao, Y., Chen, X., Zhou, H., Yang, Y., Zhang, X., Huang, Y., Zhang, N., Lui, E.M. K., Xiao, M., 2021. Pu-erh tea ameliorates obesity and modulates gut microbiota in high fat diet fed mice. Food Res. Int. 144, 110360 https://doi.org/10.1016/j.foodres.2021.110360.

Zhang, Q., Fan, X.Y., Guo, W.L., Cao, Y.J., Lin, Y.C., Cheng, W.J., Chen, L.J., Rao, P.F., Ni, L., Lv, X.C., 2020. The protective mechanisms of macroalgae Laminaria japonica consumption against lipid metabolism disorders in high-fat diet-induced hyperlipidemic rats. Food Funct. 11, 3256–3270. https://doi.org/10.1039/d0fo00065e.

Zhang, S.Q., Zhang, H.-B., Zhang, Y., 2018. Quantification of selenomethionine in plasma using UPLC–MS/MS after the oral administration of selenium-enriched yeast to rats. Food Chem. 241, 1–6. https://doi.org/10.1016/j.foodchem.2017.08.068.

Zhang, X.G., Wang, N., Ma, G.-D., Liu, Z.Y., Wei, G.-X., Liu, W.J., 2021. Preparation of S-iron-enriched yeast using siderophores and its effect on iron deficiency anemia in rats. Food Chem. 365, 130508 https://doi.org/10.1016/j.foodchem.2021.130508.

Zhao, H., Wu, H., Duan, M., Liu, R., Zhu, Q., Zhang, K., Wang, L., 2021a. Cinnamaldehyde improves metabolic functions in streptozotocin-induced diabetic mice by regulating gut microbiota. Drug Des. Dev. Ther. 15, 2339–2355. https://doi.org/10.2147/DDDT.S288011.

Zhao, T., Zhan, L., Zhou, W., Chen, W., Luo, J., Zhang, L., Weng, Z., Zhao, C., Liu, S., 2021b. The effects of erchen decoction on gut microbiota and lipid metabolism disorders in Zucker diabetic fatty rats. Front. Pharmacol. 12, 647529 https://doi.org/10.3389/fphar.2021.647529.

Zhou, F., Wu, X., Pinos, I., Abraham, B.M., Barrett, T.J., von Lintig, J., Fisher, E.A., Amengual, J., 2020. β-Carotene conversion to vitamin A delays atherosclerosis progression by decreasing hepatic lipid secretion in mice. J. Lipid Res. 61, 1491–1503. https://doi.org/10.1194/jlr.RA120001066.